Faddeev calculations of proton-deuteron radiative capture with exchange currents

J. Golak,[1,2] H. Kamada,[2,*] H. Witała,[1] W. Glöckle,[2] J. Kuroś-Zołnierczuk,[1] R. Skibiński,[1] V. V. Kotlyar,[3] K. Sagara,[4] and H. Akiyoshi[5]

[1]*Institute of Physics, Jagellonian University, PL-30059 Cracow, Poland*

[2]*Institut für Theoretische Physik II, Ruhr Universität Bochum, D-44780 Bochum, Germany*

[3]*National Science Center, ''Kharkov Institute of Physics and Technology,'' Institute of Theoretical Physics, Kharkov 310108, Ukraine*

[4]*Department of Physics, Kyushu University, Hakozaki, Fukuoka 812, Japan*

[5]*RIKEN, 2-1 Hirosawa, Wako, Saitama 351-0198, Japan*

(Received 23 June 2000; published 16 October 2000)

pd capture processes at various energies have been analyzed based on solutions of three-nucleon (3*N*)-Faddeev equations and using modern *NN* forces. The application of the Siegert theorem is compared to the explicit use of π- and ρ-like exchange currents connected to the AV18 *NN* interaction. Overall good agreement with cross sections and spin observables has been obtained but leaving room for improvement in some cases. Feasibility studies for three-nucleon forces (3NF's) consistently included in the 3N continuum and the 3N bound state have been performed as well.

PACS number(s): 21.45.+v, 24.70.+s, 25.10.+s, 25.40.Lw

I. INTRODUCTION

Recently new nucleon-nucleon (*NN*) potentials have been worked out, which describe the rich *NN* data base below the pion threshold perfectly well. This set of new potentials, often called a new generation of interactions, comprises Nijm I and Nijm II [1], AV18 [2] and CD-Bonn [3]. Used in three-nucleon (3*N*) scattering calculations they describe many observables rather well, especially at lower nucleon lab energies below about 100 MeV [4]. An important insight thereby is the robustness of that picture: the four *NN* force predictions are very close together. This allows, in case of discrepancies to data, to think that very likely one will see three-nucleon force (3NF) effects. Indeed there is increasing evidence that certain discrepancies of data and *NN* force predictions can be cured by adding 3NF's [5]. Good examples are the minima of the differential cross sections in elastic *pd* scattering at intermediate energies [6] or the deuteron vector analyzing power in the same process [7]. There are also counter examples which clearly demonstrate that the correct spin structure of 3NF's has not yet been fully established. A most prominent example is the analyzing power in elastic *pd* scattering at low and intermediate energies [8,9]. In any case these results form a solid basis to study electron scattering and photodisintegration of ^{3}He or the *pd*-capture processes, since the dynamics before and after the photon has been absorbed is fairly well under control. Though 3NF effects are of great interest and very likely certain signatures have already been identified as pointed out, by far the most 3*N* observables can to a large extent be well described by *NN* forces only. Also in view of applications to electromagnetic processes it is very important to say that the ^{3}He bound state as well as the 3*N* scattering states can reliably be calculated for one and the same Hamiltonian based on that set of new realistic *NN* forces.

Now the new dynamical ingredient for electromagnetic processes is the nuclear electromagnetic current operator. Its dependence on the electromagnetic nucleon form factors in the case of the single nucleon current and its consistency to the chosen nuclear forces are of central interests. Thus the nuclear matrix elements depending on the electromagnetic current operator allow access to the electromagnetic neutron form factors in the case of polarized ^{3}He targets [10–12] and mesonic exchange currents (MEC's) provide important insight into the nuclear dynamics.

In this paper we concentrate on effects of MEC's for the 3*N* system, which for the bound and scattering states is fully treated by solving corresponding Faddeev equations [13,14]. Our techniques to handle MEC's adapted to our general formalism is described in [15]. For low photon momenta and processes with real photons the Siegert theorem in a long-wavelength approximation [16] is quite popular and includes some of the two-body currents. We shall also use it in a form which does not rely on such an approximation and we shall compare those results to calculations using directly MEC's. As expected the comparison will look different for low and high energies.

In the long-wavelength approximation the Siegert theorem allows one to write the interaction Hamiltonian in terms of the strengths of electric and magnetic fields, i.e., in a gauge-independent form. The Siegert theorem has been extended before [17] beyond the long-wavelength approximation. Diverse aspects and properties of the Siegert-like transformations are studied in the above-mentioned references and in [18].

We compare our theory to several recent and older data. Among them are precise analyzing power data taken at the Kyushu University tandem accelerator laboratory by using an intense *d* beam and a hydrogen gas target of fairly high pressure and by detecting ^{3}He particles instead of γ rays in order to simultaneously measure the whole angular distribution [19].

In theory this field has been actively investigated before by many groups. For the older calculations we refer to [20] for an overview. More recently Torre [21] performed for a

*Present address: Institut für Strahlen- und Kernphysik der Universität Bonn, Nussallee 14-16, D-53115 Bonn, Germany.

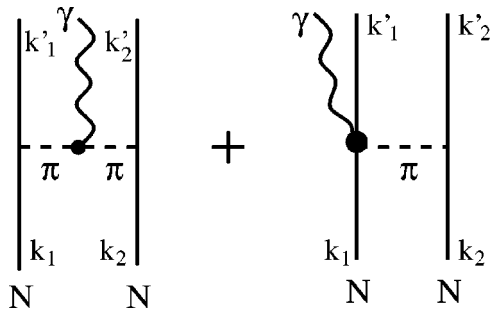

FIG. 1. The ''pion-in-flight'' and ''seagull'' pionic exchange currents.

pd capture reaction a very advanced calculation treating initial and final 3*N* states correctly and including MEC's. Ishikawa and Sasakawa [22] even included 3*N* forces for such a process. Further, based on finite rank approximations of *NN* forces Fonseca and Lehman [23] studied intensively various *pd* capture reactions. At very low energies there exist highly advanced *pd* capture calculations by Friar *et al.* [24] and Kievsky *et al.* [25], which has been reviewed recently in [26]. More recently new investigations on photodisintegration and *pd* capture appeared for very low energies in [27,28].

Our aim is to use modern forces, keep at least approximate consistency between MEC's and the nuclear forces according to the Riska prescription [29], analyze more data also at intermediate energies, and compare the results based on Siegert theorem and on the explicit use of MEC's. We also do not restrict ourselves to low multipoles as in most of the previous work.

In Sec. II we rephrase the Siegert theorem working only in momentum space. We think this is a very transparent and algebraically simple notation in contrast to the rather tedious algebraic steps usually presented in a configuration space notation [30]. It also does not require long-wavelength approximations. In that context we also want to show the connection between the partial wave representation of our former work [31] and the multipole expansion. There are many kinds of MEC's. In this paper we concentrate on π- and ρ-like exchange currents linked to the specific AV18 *NN* force. This is outlined in Sec. III. Then in Sec. IV we show

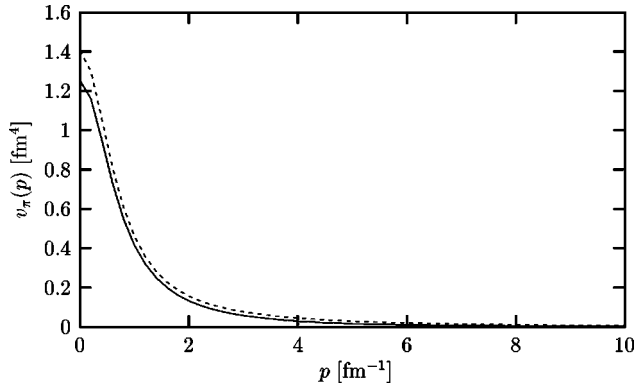

FIG. 2. Comparison of the form factors v_π for AV18 (solid line) and AV14 (dashed line).

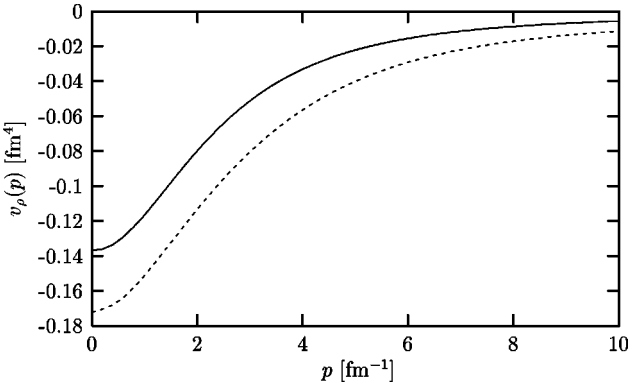

FIG. 3. Same as in Fig. 2 for v_ρ.

our way to include a 3NF force into *pd* capture calculations. The broad set of numerical results compared to data is shown in Sec. V. In a future work we shall compare the different modern *NN* force predictions with properly related MEC's in order to investigate whether this dynamical scenario is robust against interchanges of the forces. Finally we summarize in Sec. VI.

II. SIEGERT THEOREM AND MULTIPOLE EXPANSION

Multipole expansions have a long history and are a natural tool to characterize radiative transitions between the numerous levels of nuclei. In the 3*N* system there is only one bound state for ^{3}He(^{3}H) and thus no obvious need for that notation. Also working not only at very low energies very many multipoles are involved and we hardly used that notation up to now, see, however, [32]. The Siegert theorem [16] is embedded in that notation of multipoles and that theorem is very powerful in the description of *pd* capture or the photodisintegration processes. Therefore in order to apply it we want to exhibit the connection between our partial wave decomposition [31] and the multipole expansion. At the same time we want to present a short outline leading to Siegert's theorem carried through in momentum space. Work along this line has been presented before in [33,34].

The nuclear matrix element for photodisintegration of ^{3}He is

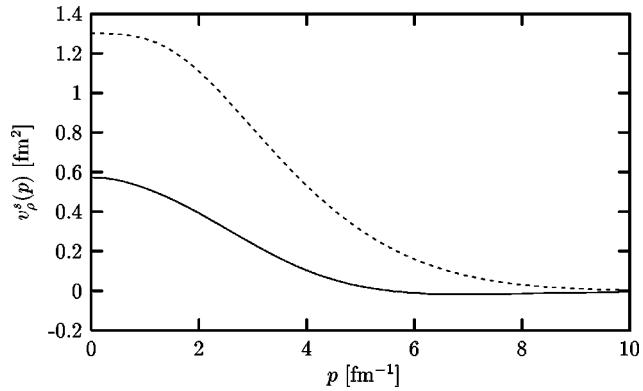

FIG. 4. Same as in Fig. 2 for v^s_ρ.

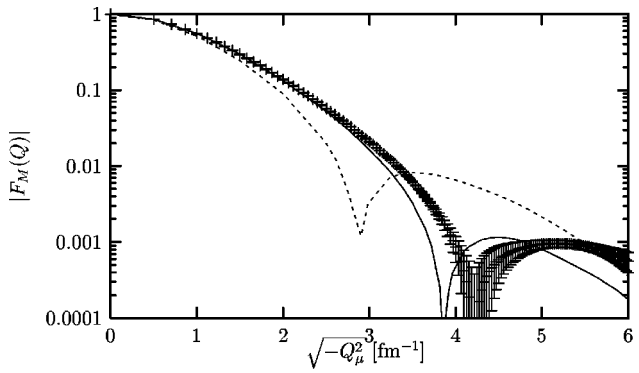

FIG. 5. The magnetic form factor of ^{3}He. The solid line includes MEC (see text), while the dashed line is based on a single-nucleon current study. Data are from [45].

$$\mathcal{J}_\xi(\vec{Q}) = \langle \vec{P}' \Psi_f^{(-)} | \vec{\epsilon}_\xi(\vec{Q}) \cdot \vec{j}(0) | \Psi_{^3\mathrm{He}} \vec{P} \rangle \equiv \vec{\epsilon}_\xi(\vec{Q}) \cdot \vec{I}(\vec{Q}), \tag{1}$$

where $\Psi_{^3\mathrm{He}}$ and $\Psi_f^{(-)}$ are $3N$ bound and scattering states, $\vec{P}$ and $\vec{P}'$ are the total $3N$ momenta before and after photon absorption, $\vec{\epsilon}_\xi(\vec{Q})$ is a spherical component of the photon polarization vector, and $\vec{j}(0)$ is the nuclear current operator. It consists in general of a single nucleon part and more than one nucleon parts. The three components of the nuclear matrix element $\vec{I}(\vec{Q})$ can be expanded into spherical harmonics. Choosing the photon direction $\hat{Q}$ to point in the $\hat{z}$ direction we expand the product of the polarization vector $\vec{\epsilon}_\xi(\vec{z})$ and the spherical harmonics $Y_{l0}(\hat{Q}')$ into vector spherical harmonics. This then leads immediately to

$$\begin{aligned} \vec{\epsilon}_\xi(\vec{z}) \cdot \vec{I}(|\vec{Q}|\hat{z}) &= \frac{1}{2\sqrt{\pi}} \sum_{J \geqslant 1} \sum_{l=J,J\pm 1} \sqrt{2l+1} C(l1J,0\xi) \\ &\quad \times \int d\hat{Q}' \vec{Y}^\xi_{Jl1}(\hat{Q}) \cdot \vec{I}(|\vec{Q}|\hat{Q}') \\ &\equiv -\sqrt{2\pi} \sum_{J\sigma} \xi^\sigma \sqrt{2J+1}\ T^\sigma_{J\xi}(|\vec{Q}|), \end{aligned} \tag{2}$$

which is the usual multipole expansion. Inserting the Clebsch-Gordan coefficients one gets

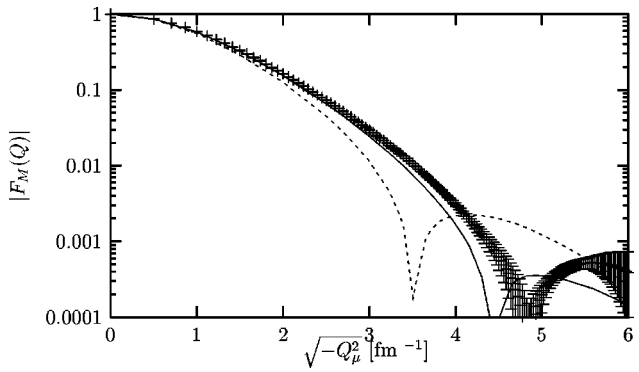

FIG. 6. Same as in Fig. 5 for ^{3}H. Data are from [45].

TABLE I. Proton and deuteron lab energies and corresponding photon momenta for the inverse reaction in the lab system for experiments analyzed in this work.

E_p MeV	E_d MeV	Q MeV/c
5.0	10.0	8.8
8.8	17.5	11.4
9.9	19.8	12.1
14.8	29.6	15.4
22.5	45.0	20.5
47.5	95.0	37.2
100.0	199.9	72.3
150.0	299.9	105.7
200.0	399.8	139.1

$$T^{\sigma=0}_{J\xi}(Q) \equiv T^{el}_{J\xi}(Q) = -\frac{1}{4\pi} \int d\hat{Q}' \left\{ \sqrt{\frac{J}{2J+1}} \vec{Y}^\xi_{JJ+11}(\hat{Q}) + \sqrt{\frac{J+1}{2J+1}} \vec{Y}^\xi_{JJ-11}(\hat{Q}') \right\} \cdot \vec{I}(|\vec{Q}|\hat{Q}') \tag{3}$$

and

$$T^{\sigma=1}_{J\xi}(Q) \equiv T^{mag}_{J\xi}(Q) = \frac{1}{4\pi} \int d\hat{Q}' \vec{Y}^\xi_{JJ1}(\hat{Q}') \cdot \vec{I}(|\vec{Q}|\hat{Q}'). \tag{4}$$

This separates the magnetic multipoles $T^{mag}_{J\xi}$ $(l=J)$ and the electric multipoles $T^{el}_{J\xi}$ $(l=J\pm 1)$. Now we use the identity [35]

$$\hat{Q} Y_{J\xi}(\hat{Q}) = -\sqrt{\frac{J+1}{2J+1}} \vec{Y}^\xi_{JJ+11}(\hat{Q}) + \sqrt{\frac{J}{2J+1}} \vec{Y}^\xi_{JJ-11}(\hat{Q}), \tag{5}$$

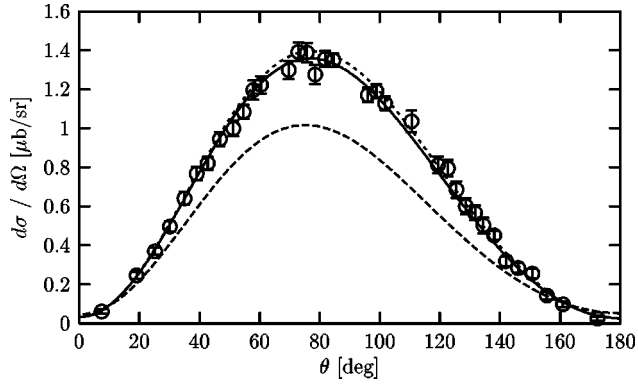

FIG. 7. The photon angular distribution for pd capture at $E_d = 19.8$ MeV against the c.m. γ-p scattering angle. The single nucleon current prediction is given by the dashed line, including MEC leads to the solid line, and the dotted line is due to Siegert. Data are from [47].

which allows us to rewrite the term with $\vec{Y}^{\xi}_{JJ-11}(\hat{Q})$ in terms of $\vec{Y}^{\xi}_{JJ+11}(\hat{Q})$ and most importantly the term $\hat{Q}Y_{J\xi}(\hat{Q})$. On the other hand $\hat{Q}\cdot\vec{I}(\vec{Q})$ occurs in the continuity equation for the electromagnetic current

$$\begin{aligned}\vec{Q}\cdot\vec{I}(\vec{Q}) &= \langle \vec{P}'\Psi^{(-)}_{f'}|[H,\hat{\rho}(0)]|\Psi_{^3\mathrm{He}}\vec{P}\rangle \\ &= \langle \vec{P}'\Psi^{(-)}_{f'}|(E'\hat{\rho}(0)-\hat{\rho}(0)E)|\Psi_{^3\mathrm{He}}\vec{P}\rangle \\ &= \omega\langle \vec{P}'\Psi^{(-)}_{f'}|\hat{\rho}(0)|\Psi_{^3\mathrm{He}}\vec{P}\rangle \\ &\equiv Q\rho(\vec{Q}) \end{aligned} \tag{6}$$

with

$$|\vec{Q}| = Q = \omega. \tag{7}$$

Therefore, we end up for the electric multipoles with

$$T^{el}_{J\xi}(Q) \equiv -\frac{1}{4\pi}\int d\hat{Q}'\left\{\sqrt{\frac{2J+1}{J}}\vec{Y}^{\xi}_{JJ+11}(\hat{Q}')\cdot\vec{I}(|\vec{Q}|\hat{Q}') + \sqrt{\frac{J+1}{J}}Y_{J\xi}(\hat{Q}')\rho(|\vec{Q}|\hat{Q}')\right\}. \tag{8}$$

Another derivation of that formula is presented in the Appendix. Note that the first term in the curly bracket in Eq. (8) is normally neglected in a long-wavelength approximation. The last term is now the density matrix element, which is believed to be less affected (at least for low momenta) by two-body effects. Therefore a single body operator might be a reasonable approximation. In this paper we use that assumption and keep also the first term, however in a single nucleon current approximation. In the result section we refer by ''Siegert'' to such a choice. Thus the identity given in Eq. (5) together with current conservation and exact $3N$ eigenstates of the Hamiltonian H allowed us to shift the effects of the unknown current matrix element $\vec{I}(\vec{Q})$ into $\rho(\vec{Q})$ and into higher multipoles. Clearly this is only a first step towards introducing two-body currents.

Now let us indicate in the example of the single nucleon density operator the connection between our partial wave expansion and the multipole expansion. Working in momentum space and in a partial wave decomposition for three nucleons we use the basis $|pq\beta\rangle$, where p and q are the magnitudes of Jacobi momenta and β a set of discrete quantum numbers (orbital and spin angular momenta coupled to the total $3N$ angular momentum and isospin quantum numbers) [31].

The density matrix element has the structure

$$\rho(\vec{Q}) = \sum\!\!\!\!\!\!\int \langle\Psi^{(-)}_f|pq\beta\rangle\langle pq\beta|\hat{\rho}(\vec{Q})|\Psi_{^3\mathrm{He}}\rangle. \tag{9}$$

For our purpose it is sufficient to regard only $\langle pq\beta|\hat{\rho}(\vec{Q})|\Psi_{^3\mathrm{He}}\rangle$, which is shown in [31] to have the form for a single nucleon density operator

$$\begin{aligned}\left\langle pq\beta(\mathcal{J}M)|\hat{\rho}(\vec{Q}\|\hat{z})|\Psi_{bound}\left(\frac{1}{2}M'\right)\right\rangle &= \delta_{M,M'}\delta_{M_T,M_{T'}}\frac{1}{2}\sqrt{\hat{\mathcal{J}}}\sqrt{\hat{L}}(-1)^{S+\mathcal{J}}[I^{(p)}(t,T,M_T)F^p_1(\vec{Q})+I^{(n)}(t,T,M_T)F^n_1(\vec{Q})] \\ &\times\sum_{\beta'}\ \delta_{l,l'}\delta_{s,s'}\delta_{S,S'}\delta_{t,t'}\sqrt{\hat{\lambda}'\hat{L}'}\sum_{\lambda_1+\lambda_2=\lambda'}\ \sqrt{\frac{(2\lambda'+1)!}{(2\lambda_1)!(2\lambda_2)!}}q^{\lambda_1}\left(\frac{2}{3}Q\right)^{\lambda_2} \\ &\times\sum_k\ \hat{k}C(\lambda_1,k,\lambda;0,0,0)\int_{-1}^{1}dxP_k(x) \\ &\times\frac{\langle p\tilde{q}\beta'|\Psi_{bound}\rangle}{\tilde{q}^{\lambda'}}\sum_g\ \sqrt{\hat{g}}\ C(\lambda_2,k,g;0,0,0)\begin{Bmatrix}\lambda_2 & \lambda_1 & \lambda'\\ \lambda & g & k\end{Bmatrix}\begin{Bmatrix}l & \lambda & L\\ g & L' & \lambda'\end{Bmatrix} \\ &\times\begin{Bmatrix}\mathcal{J} & L & S\\ L' & \frac{1}{2} & g\end{Bmatrix}C\left(\mathcal{J},g,\frac{1}{2};M,0,M'\right).\end{aligned} \tag{10}$$

We also indicated now in the bra vector explicitly the total $3N$ angular momentum $\mathcal{J}$ and its magnetic quantum number M. Here it is assumed that $\hat{Q}=\hat{z}$. On the other hand, the part of the electric multipole related to ρ in Eq. (8) is

$$T^{el;\rho}_{J\xi} \equiv -\frac{1}{4\pi}\int d\hat{Q}'\sqrt{\frac{J+1}{J}}Y_{J\xi}(\hat{Q}')\rho(|\vec{Q}|\hat{Q}'). \tag{11}$$

In order to perform the integral in Eq. (11) we need the generalization of Eq. (10) to an arbitrary $\hat{Q}$ direction. This is easily achieved by replacing in Eq. (10) $\delta_{M,M'}C(\mathcal{J},g,\frac{1}{2};M,0,M')$ by

$$\sqrt{\frac{4\pi}{\hat{g}}}Y_{g,M'-M}(\hat{Q})C\left(\mathcal{J},g,\frac{1}{2};M,M'-M,M'\right). \tag{12}$$

Then the integral can be performed and one ends up with

$$T^{el;\rho}_{J\xi}=\sum\!\!\!\!\!\!\int \langle\Psi^{(-)}_{\vec{f}}|pq\beta\rangle\langle pq\beta|\Phi^{el;\rho}_{J\xi}\rangle, \tag{13}$$

where $\langle pq\beta|\Phi^{el;\rho}_{J\xi}\rangle$ is given by

$$\begin{aligned}\langle pq\beta|\Phi^{el;\rho}_{J\xi}\rangle=&\delta_{M_T,M_{T'}}\frac{1}{4}\frac{1}{\sqrt{\pi}}\sqrt{\frac{J+1}{J}}(-1)^{\xi}C\left(\mathcal{J},J,\frac{1}{2};M,-\xi,M'\right)\begin{Bmatrix} l & \lambda & L\\ J & L' & \lambda'\end{Bmatrix}\begin{Bmatrix} \mathcal{J} & L & S\\ L' & \frac{1}{2} & J\end{Bmatrix}\\ &\times\sqrt{\hat{\mathcal{J}}}\sqrt{\hat{L}}(-1)^{S+\mathcal{J}}[I^{(p)}(t,T,M_T)F_1^p(\vec{Q})+I^{(n)}(t,T,M_T)F_1^n(\vec{Q})]\sum_{\beta'}\delta_{l,l'}\delta_{s,s'}\delta_{S,S'}\delta_{t,t'}\sqrt{\hat{\lambda}'\hat{L}'}\\ &\times\sum_{\lambda_1+\lambda_2=\lambda'}\sqrt{\frac{(2\lambda'+1)!}{(2\lambda_1)!(2\lambda_2)!}}q^{\lambda_1}\left(\frac{2}{3}Q\right)^{\lambda_2}\sum_k \hat{k}C(\lambda_1,k,\lambda;0,0,0)C(\lambda_2,k,J;0,0,0)\\ &\times\begin{Bmatrix}\lambda_2 & \lambda_1 & \lambda'\\ \lambda & J & k\end{Bmatrix}\int_{-1}^{1}dxP_k(x)\frac{\langle p\tilde{q}\beta'|\Psi_{bound}\rangle}{\tilde{q}^{\lambda'}}.\end{aligned} \tag{14}$$

As a consequence the variable g in Eq. (10) has to be identified with J—the multipole order of Eq. (14). A corresponding relation can easily be worked out for the remaining parts in Eqs. (8) and (4).

III. MODEL OF MESON EXCHANGE CURRENTS

The study of meson-exchange currents has also a long history. We follow the scheme adopted by the Urbana-Argonne Collaboration [26], based on the Riska prescription [29]. Dominant contributions arise from the π and ρ exchanges, to which we restrict ourselves in this paper. The π current consists of the so-called seagull and pion in flight parts, which in case of a true pion exchange are displayed in Fig. 1. The well-known expressions are

$$\begin{aligned}\vec{j}^{seagull}(\vec{p}_1,\vec{p}_2)\equiv& i[\tau(1)\times\tau(2)]_z F_1^V[v_\pi(p_1)(\vec{\sigma}(1)\cdot\vec{p}_1)\vec{\sigma}(2)\\ &-v_\pi(p_2)(\vec{\sigma}(2)\cdot\vec{p}_2)\vec{\sigma}(1)],\end{aligned}$$

$$\begin{aligned}\vec{j}^{pionic}(\vec{p}_1,\vec{p}_2)\equiv& i[\tau(1)\times\tau(2)]_z F_1^V(\vec{p}_1-\vec{p}_2)[\vec{\sigma}(1)\cdot\vec{p}_1]\\ &\times[\vec{\sigma}(2)\cdot\vec{p}_2]\frac{v_\pi(p_2)-v_\pi(p_1)}{p_1^2-p_2^2},\end{aligned} \tag{15}$$

where $\vec{p}_1$ and $\vec{p}_2$ are defined in terms of the initial and final momenta as

$$\begin{aligned}\vec{p}_1\equiv&\vec{k}_1{}'-\vec{k}_1,\\ \vec{p}_2\equiv&\vec{k}_2{}'-\vec{k}_2.\end{aligned} \tag{16}$$

Further F_1^V is the isovector electromagnetic nucleon form factor. In the case of just a pion exchange and dropping the strong form factors $v_\pi(p)$ is given as

$$v_\pi(p)=\frac{f^2_{\pi NN}}{m^2_\pi}\frac{1}{m^2_\pi+p^2}, \tag{17}$$

where $f_{\pi NN}$ and m_π are the pseudovector πNN coupling constant and the pion mass, respectively. Similarly the ρ current is given as

$$\vec{j}^{\rho}_{12}\equiv\vec{j}_{\rho,I}+\vec{j}_{\rho,II}+\vec{j}_{\rho,III}+\vec{j}_{\rho,IV}, \tag{18}$$

$$\begin{aligned}\vec{j}_{\rho,I}(\vec{p}_1,\vec{p}_2)\equiv& i[\vec{\tau}(1)\times\vec{\tau}(2)]_z F_1^V(Q^2)\frac{\vec{p}_1-\vec{p}_2}{p_1^2-p_2^2}\\ &\times[v^S_\rho(p_2)-v^S_\rho(p_1)],\end{aligned}$$

$$\begin{aligned}\vec{j}_{\rho,II}(\vec{p}_1,\vec{p}_2)\equiv&-i[\vec{\tau}(1)\times\vec{\tau}(2)]_z F_1^V(Q^2)[v_\rho(p_2)\,\vec{\sigma}(1)\\ &\times(\vec{\sigma}(2)\times\vec{p}_2)-v_\rho(p_1)\,\vec{\sigma}(2)\times(\vec{\sigma}(1)\times\vec{p}_1)],\end{aligned}$$

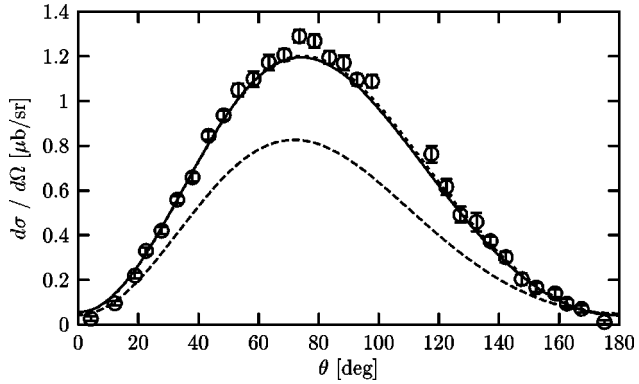

FIG. 8. The same as in Fig. 7 at $E_d=29.6$ MeV. Note that the calculations are for $E_d=29.2$ MeV. Data are from [47].

$$\vec{j}_{\rho,III}(\vec{p}_1,\vec{p}_2)\equiv -i[\vec{\tau}(1)\times\vec{\tau}(2)]_z F_1^V(Q^2) \times\frac{v_\rho(p_2)-v_\rho(p_1)}{p_1^2-p_2^2} \times[(\vec{\sigma}(1)\times\vec{p}_1)\cdot(\vec{\sigma}(2)\times\vec{p}_2)](\vec{p}_1-\vec{p}_2)\,,$$

$$\vec{j}_{\rho,IV}(\vec{p}_1,\vec{p}_2)\equiv -i[\vec{\tau}(1)\times\vec{\tau}(2)]_z F_1^V(Q^2)\frac{v_\rho(p_2)-v_\rho(p_1)}{p_1^2-p_2^2} \times[\vec{\sigma}(2)\cdot(\vec{p}_1\times\vec{p}_2)(\vec{\sigma}(1)\times\vec{p}_1) +\vec{\sigma}(1)\cdot(\vec{p}_1\times\vec{p}_2)(\vec{\sigma}(2)\times\vec{p}_2)].$$

Again for just a ρ exchange one would have

$$v_\rho(k)=-\left(\frac{g_{\rho NN}}{2m_N}\right)^2\frac{(1+\kappa)^2}{m_\rho^2+k^2},$$

$$v_\rho^S(k)=g_{\rho NN}^2\frac{1}{m_\rho^2+k^2}, \tag{19}$$

where $g_{\rho NN}$, κ, and m_ρ are the vector, tensor ρNN coupling constants, and the ρ meson mass, respectively. Now according to Riska's prescription one identifies π- and ρ-like parts

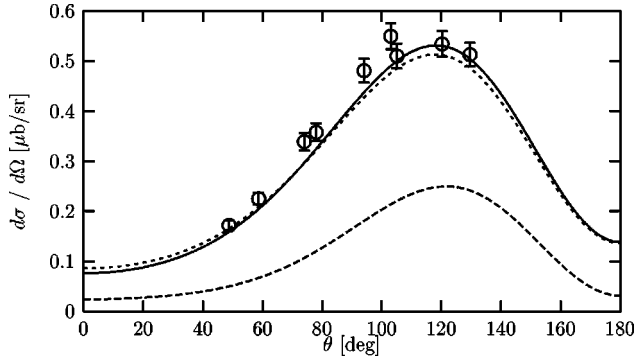

FIG. 9. The same as in Fig. 7 at $E_d=95$ MeV. θ is the c.m. γ-d scattering angle. Data are from [48].

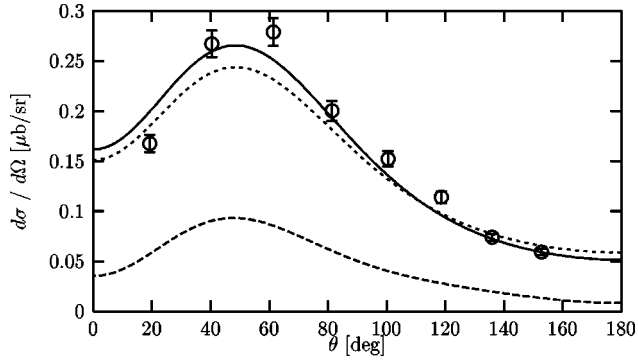

FIG. 10. The same as in Fig. 7 at $E_p=100$ MeV. θ is the c.m. γ-p scattering angle. Data are from [49].

in the given NN potential and using the continuity equation finds a linkage of the potential to the exchange currents. The procedure is as follows:

$$v_\pi(k)\rightarrow v_{PS}(k)=2v^{t\tau}(k)-v^{\sigma\tau}(k), \tag{20}$$

$$v_\rho(k)\rightarrow v_V(k)=v^{t\tau}(k)+v^{\sigma\tau}(k), \tag{21}$$

and

$$v_\rho^S(k)\rightarrow v_V^S(k)=v^\tau(k), \tag{22}$$

where the functions $v_{PS}(k)$, $v_V(k)$, $v_V^S(k)$ are evaluated as

$$v^{\sigma\tau}(k)=\frac{4\pi}{k^2}\int_0^\infty drr^2[j_0(kr)-1]v^{\sigma\tau}(r), \tag{23}$$

$$v^{t\tau}(k)=\frac{4\pi}{k^2}\int_0^\infty drr^2 j_2(kr)v^{t\tau}(r), \tag{24}$$

$$v^\tau(k)=4\pi\int_0^\infty drr^2 j_0(kr)v^\tau(r). \tag{25}$$

The functions $v^{\sigma\tau}(r)$, $v^{t\tau}(r)$, $v^\tau(r)$ are taken from the AV18 potential and are the radial functions accompanying the spin-isospin, tensor-isospin, and isospin operators, respectively. It is interesting to look at the potential-dependent

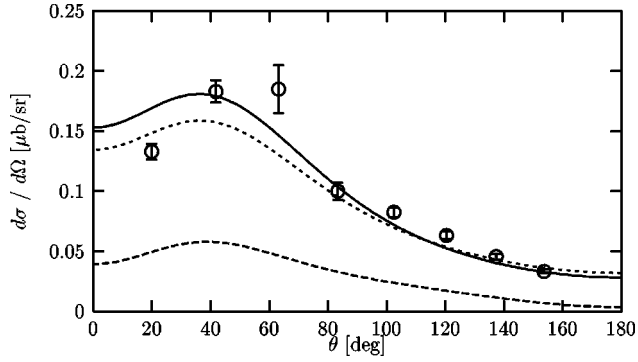

FIG. 11. The same as in Fig. 7 at $E_p=150$ MeV. θ is the c.m. γ-p scattering angle. Data are from [49].

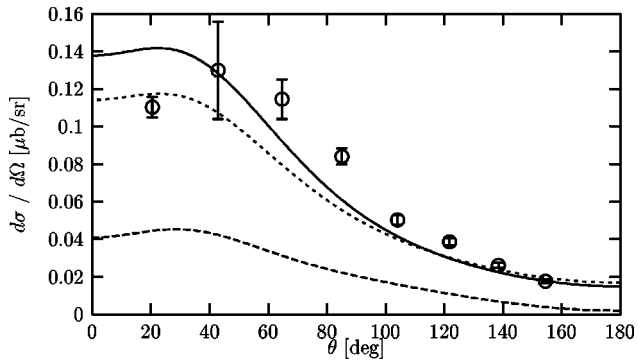

FIG. 12. The same as in Fig. 7 at $E_p = 200$ MeV. θ is the c.m. γ-p scattering angle. Data are from [49].

functions $v_{PS}(k)$, $v_V(k)$, and $v_V^S(k)$ for different NN potentials. In Figs. 2–4 we compare them for the AV14 [36] and AV18 [2].

IV. INCLUSION OF A THREE-NUCLEON FORCE

In this section we would like to demonstrate our method of including a three-nucleon force in pd capture calculations. For the 3N bound state it has been done in [13] and also fully converged calculations are available for elastic and inelastic nucleon-deuteron scattering [4,6,7].

We apply the method proposed in [37] and start directly with the nuclear matrix element for the pd capture process:

$$\overline{\mathcal{J}}_{\vec{\xi}}(\vec{Q}) \equiv \langle \Psi_{^3\mathrm{He}} \vec{P} | \vec{\epsilon}_{\vec{\xi}}(\vec{Q}) \cdot \vec{j}(0) | \vec{P}' \Psi_f^{(+)} \rangle. \tag{26}$$

The scattering state $\Psi_f^{(+)}$ is then split into three Faddeev components, which for a system of identical particles reads

$$\Psi_f^{(+)} = \psi_1 + \psi_2 + \psi_3 = (1 + P_{12}P_{23} + P_{13}P_{23})\psi_1 \equiv (1+P)\psi_1. \tag{27}$$

The Faddeev component ψ fulfills the following equation (we drop the index 1):

$$\psi = \phi + G_0 t P \psi + (1 + G_0 t) G_0 V_4^{(1)} (1+P) \psi. \tag{28}$$

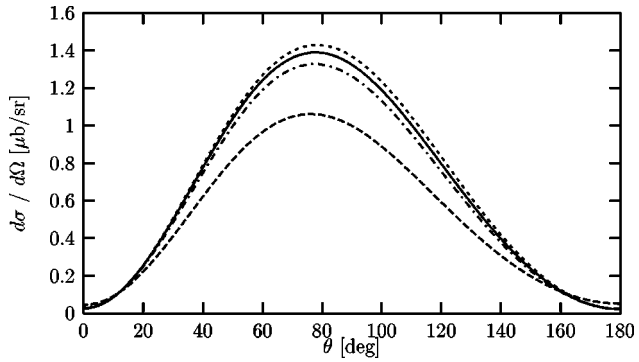

FIG. 13. The ^{3}He angular distribution for pd capture at $E_d = 17.5$ MeV against the c.m. ^{3}He-d scattering angle. The curves describe the single nucleon current (dashed), the single nucleon plus the π-MEC (dashed-dotted), the single nucleon plus the π- and ρ-MEC (solid), and Siegert (dotted) predictions.

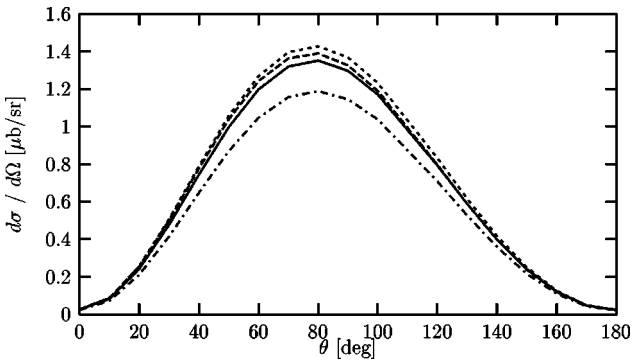

FIG. 14. The ^{3}He angular distribution for pd capture at $E_d = 17.5$ MeV against the c.m. ^{3}He-d scattering angle. The curves describe the Siegert prediction without 3NF (dotted), the Siegert prediction including 3NF (dashed-dotted), the single nucleon plus MEC without 3NF (dashed), and the single nucleon plus MEC including the 3NF (solid) predictions.

Here G_0 is the free 3N propagator, t is the off-shell NN t operator, and ϕ is a product of the deuteron state and a momentum eigenstate of the spectator nucleon. $V_4^{(1)}$ results from the decomposition of a 3NF into three parts $V_4^{(i)}$, which individually are symmetrical under the exchange of particles j and k ($j \neq i$ and $k \neq i$):

$$V_4 = V_4^{(1)} + V_4^{(2)} + V_4^{(3)}. \tag{29}$$

Introducing the amplitude $\tilde{T}$, which obeys the equation [37]

$$\tilde{T} = tP\phi + (1 + tG_0)V_4^{(1)}(1+P)\phi + tPG_0\tilde{T} + (1+tG_0) \times V_4^{(1)}(1+P)G_0\tilde{T}, \tag{30}$$

we end up with

$$\psi = \phi + G_0 \tilde{T}. \tag{31}$$

Equation (30) reduces to the form

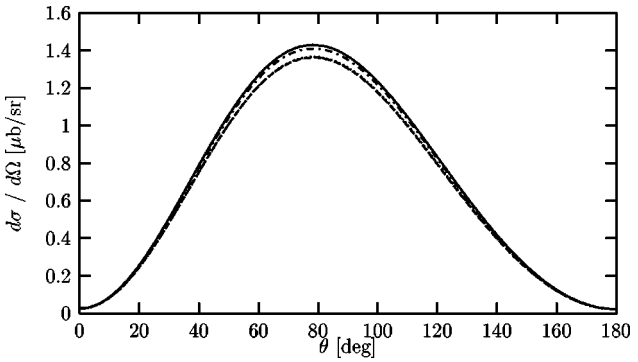

FIG. 15. The ^{3}He angular distribution for pd capture at $E_d = 17.5$ MeV against the c.m. ^{3}He-d scattering angle. The curves describe the Siegert predictions based on different NN forces: Nijm I (dotted), Nijm II (dashed-dotted), CD Bonn (dashed), and AV18 (solid).

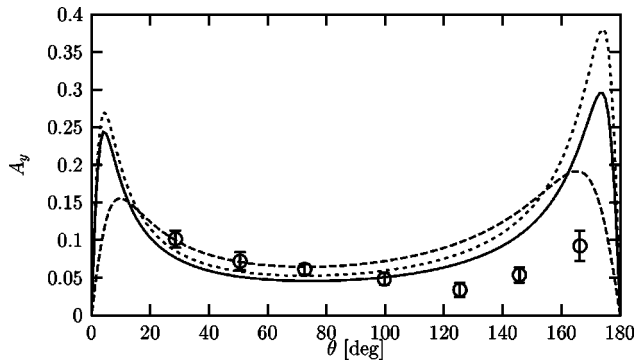

FIG. 16. The proton analyzing power $A_y(p)$ at $E_p=5$ MeV against the c.m. γ-p scattering angle. Curves as in Fig. 7. Data are from [46].

$$T=tP\phi+tPG_0T, \tag{32}$$

when the Hamiltonian contains only NN interactions ($V_4=0$).

In such a way we study 3NF effects by choosing either just the solution of Eq. (30) or Eq. (32), inserting it into Eqs. (31) and (27) and applying the nuclear current operator to the proper 3N bound-state wave function.

Thus the nuclear matrix element for the pd capture process $\overline{\mathcal{J}}_\xi(\vec{Q})$ can be split into the plane wave part and the part containing all initial-state interactions

$$\overline{\mathcal{J}}_\xi(\vec{Q})=\langle\Psi_{^3\mathrm{He}}\vec{P}|\vec{\epsilon}_\xi(\vec{Q})\cdot\vec{j}(0)|(1+P)\phi\vec{P}'\rangle + \langle\Psi_{^3\mathrm{He}}\vec{P}|\vec{\epsilon}_\xi(\vec{Q})\cdot\vec{j}(0)|(1+P)G_0\tilde{T}\vec{P}'\rangle. \tag{33}$$

V. RESULTS

Let us first repeat calculations performed before by several groups for the magnetic form factors of ^{3}He and ^{3}H. In Figs. 5 and 6 we compare the single nucleon current prediction with the one including the π- and ρ-like exchange currents. We use the AV18 potential [2] without the various electromagnetic parts. Therefore, the result of a Faddeev calculation for the ^{3}H binding energy is only 7.623 MeV. The electromagnetic nucleon form factors (G_E and G_M) are from [38]. We see the well-known strong shift of theory towards the data when including the MEC's. In this paper we restrict ourselves to relatively low photon momenta (see Table I), therefore we are not concerned about the discrepancies at the higher Q values in Figs. 5 and 6, where also relativity should play some role. In relation to the higher Q values we refer to [26,39], where theory has been pushed further including additional MEC's and Δ admixtures.

Now we come to the main results and regard first the photon angular distributions for pd capture reactions. For the current matrix element $\mathcal{J}_\xi(\vec{Q})$ defined in Eq. (1) the unpolarized cross section in the total momentum zero frame (c.m.) is given as

$$d\sigma^{\mathrm{c.m.}}=(2\pi)^2\alpha\frac{1}{|\vec{v}_d-\vec{v}_p|}\frac{1}{\omega}\frac{1}{6}\sum_{m_d,m_p,M}\sum_{\xi=\pm1}\times|\mathcal{J}_\xi(\vec{Q})|^2Q^2dQd\Omega_Q\delta(\sqrt{m^2_{^3\mathrm{He}}+Q^2}+Q-\sqrt{s}), \tag{34}$$

where α, $\vec{v}_d$, $\vec{v}_p$, and ω are the fine structure constant ($\approx1/137$), the velocities of the incident deuteron and proton, and the energy of the outgoing photon, respectively. $\sqrt{s}$ is the total energy of the $p+d$ and ^{3}He$+\gamma$ systems ($\sqrt{s}=E_d+E_p=E_{^3\mathrm{He}}+Q$). The differential cross section ($d\sigma/d\Omega_Q$) is then obtained as

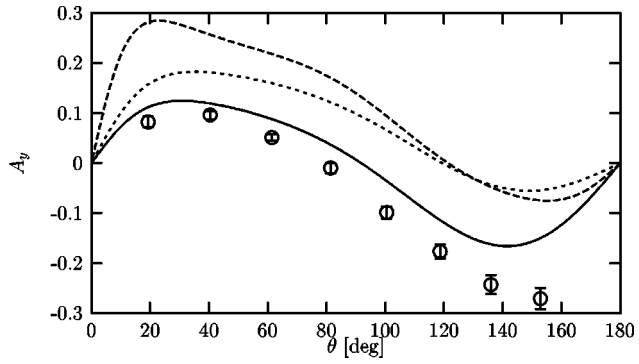

FIG. 17. The same as in Fig. 16 at $E_p=100$ MeV. Data are from [49].

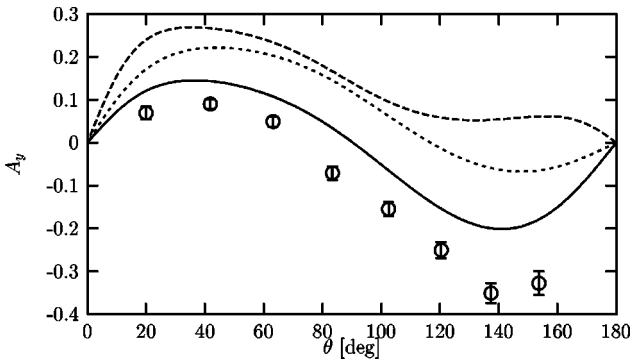

FIG. 18. The same as in Fig. 16 at $E_p=150$ MeV. Data are from [49].

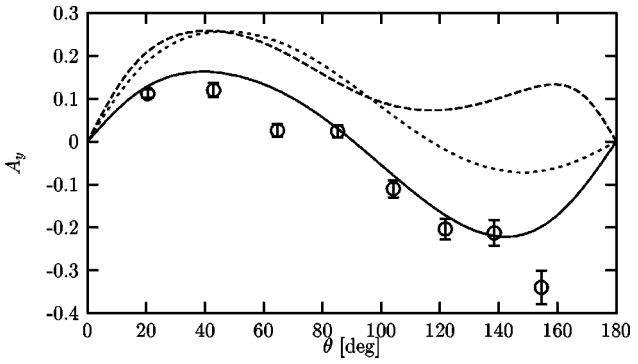

FIG. 19. The same as in Fig. 16 at $E_p=200$ MeV. Data are from [49].

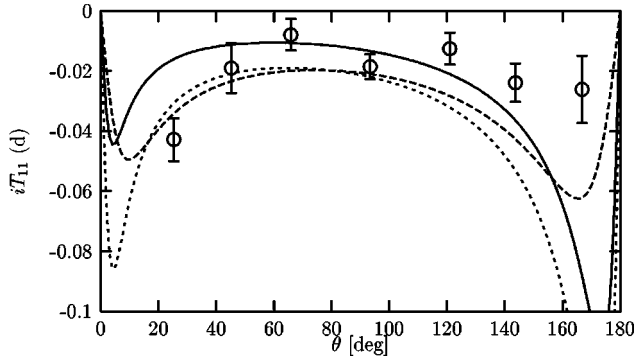

FIG. 20. The deuteron analyzing power iT_{11} at $E_d=10$ MeV against the c.m. γ-p scattering angle. Curves as in Fig. 7. Data are from [46].

$$\left(\frac{d\sigma}{d\Omega_Q}\right)^{\text{c.m.}} = (2\pi)^2\alpha\frac{1}{6}\sum_{m_d,m_p,M}\sum_{\xi=\pm 1}|\mathcal{J}_\xi(\vec{Q})|^2\frac{E_pE_dE_{^3\text{He}}Q}{s\,p_p}, \tag{35}$$

where p_p is the magnitude of the proton momentum. Note that we use the relativistic phase-space factor.

The photon angular distributions for pd capture are shown in Figs. 7–12. The single nucleon current prediction is compared to the calculations including the Siegert theorem, to the results adding the π- and ρ-like exchange currents to the single nucleon current, and to the data. We see that the single nucleon current prediction underestimates the data. Siegert and explicit MEC's are close to the data and to each other, but still leave room for improvement. At the higher energies when $E_p=100$, 150, and 200 MeV ($E_\gamma>$ 70 MeV) one may note a slight superiority of the explicit MEC prediction over the Siegert approach.

In Fig. 13 we show predictions for the ^{3}He angular distribution in the pd capture process for different choices of the electromagnetic current operator at a low energy. Apparently the Siegert choice is not fully exhausted by the electric multipole parts of the π- and ρ-like MEC's but we see that the π-exchange MEC is the dominant one of the two. An interesting insight into 3NF effects is shown in Fig. 14. We use the Tuscon-Melbourne force [40], which has been adjusted to the ^{3}He binding energy [13]. We see a relatively strong decrease of the peak height by including the 3NF in the case of the Siegert approach and a less pronounced shift in the same direction when using MEC's. In [41] it has been argued (see also [42]) that this fact is related to the ^{3}He binding energy. Apparently this can be more subtle due to the interplay with the current operator used. Finally, we display the theoretical uncertainty arising from the fact that the various NN forces do not yield the same results (Fig. 15). This spread is relatively low ($\leqslant 5\%$ in the maximum), which is satisfying in the Siegert approach. It will be very interesting to see in the future, whether different NN forces taken together with consistently applied MEC's will lead to a comparably small spread. Only if such a robustness can be demonstrated can one have some confidence in this dynamical scenario.

Let us now regard various spin observables. Nucleon analyzing powers $A_y(p)$ are shown in Figs. 16–19. At the lowest energy of 5 MeV all three theoretical predictions are close together and near the data below 100 degrees, but at extreme forward and backward angles the two calculations including two-body currents show strong enhancements, which are not seen in the data at the backward angles. Very precise data especially at those extreme angles would be of interest to put higher pressure on the theory. At the three higher energies the explicit use of MEC's is clearly much closer to the data than the Siegert approach and clearly the single nucleon current alone is not acceptable.

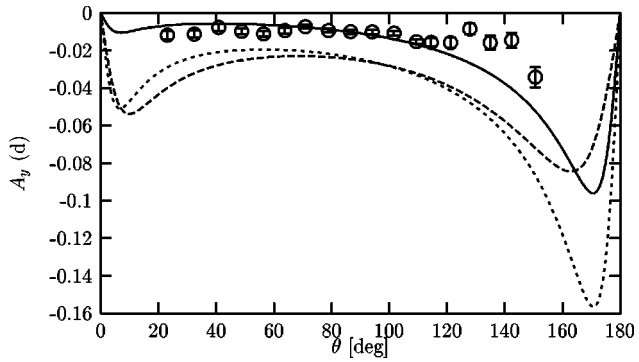

FIG. 21. The deuteron analyzing power $A_y(d)$ at $E_d=17.5$ MeV against the c.m. ^{3}He-d scattering angle. Curves as in Fig. 7. Data are from [19].

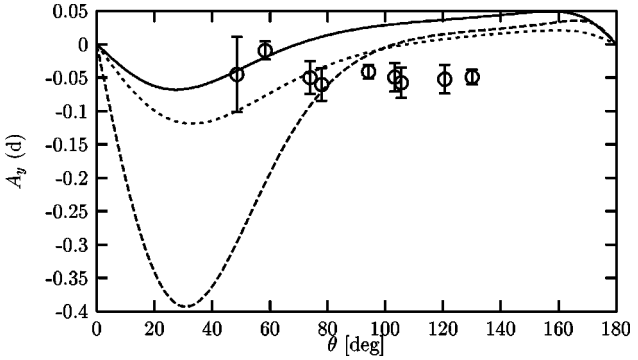

FIG. 22. The same as in Fig. 21 at $E_d=95$ MeV. θ is the c.m. γ-d scattering angle. Data are from [48].

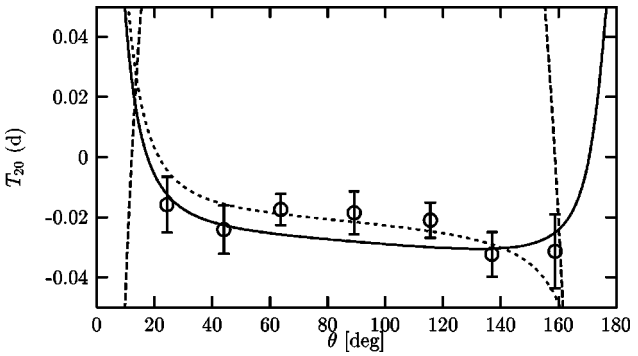

FIG. 23. The tensor analyzing power T_{20} at $E_d=10$ MeV against the c.m. γ-p scattering angle. Curves as in Fig. 7. Data are from [46].

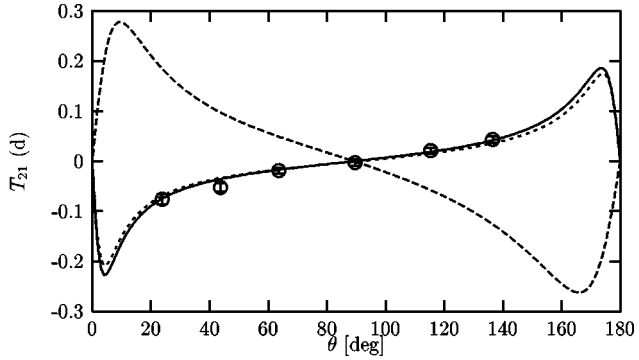

FIG. 24. The same as in Fig. 23 for the tensor analyzing power T_{21}. Data are from [46].

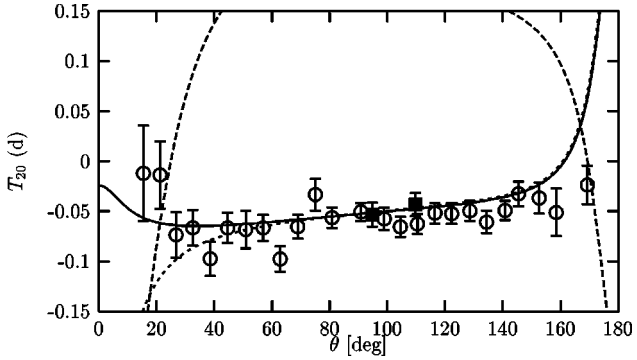

FIG. 26. The same as in Fig. 23 at $E_d=19.8$ MeV. Data are from [50] (circles) and from [51] (squares).

Our results for the deuteron vector analyzing power iT_{11} or $A_y(d)$ are shown in Figs. 20–22. The agreement with the data is in general only fair. At the lowest energy the extreme enhancement at large backward angles of the predictions including MEC or Siegert is clearly ruled out by the one data point. At $E_d=17.5$ MeV the MEC prediction appears to be reasonable, if there were not that enhancement at the large angles. At $E_d=95$ MeV Siegert and the explicit MEC are comparable, but are missing the data at backward angles.

Last but not least, we regard a rich set of tensor analyzing powers in Figs. 23–29. At $E_d=10$ MeV Siegert and MEC predictions agree for T_{20} and T_{21} and the data. For the T_{22} this is different and the data scatter a lot. We would like to point to the very different behavior of the MEC and Siegert predictions at large angles for T_{20}. The reason for that unacceptable behavior is right now open. At $E_d=19.8$ MeV this quite different behavior for MEC and Siegert predictions appears at extreme forward angles. Otherwise both predictions agree with each other and the data. At $E_d=29.2$ MeV our results (0.0326 for Siegert and 0.0315 for MEC) for the single A_{yy} data point ($\theta=96°$) of [21] agree with the calculations by Torre [21] (0.0339), although in his case the Reid soft-core potential [43] was used. A_{yy} is fairly well described for $E_d=45$ MeV and $E_d=95$ MeV. The data at $E_d=45$ MeV have been analyzed by us before using the Bonn-B potential together with the Siegert approach [32].

At $E_d=17.5$ MeV we show again in detail the various predictions. From Figs. 30–32 one can infer that the π exchange provides the strongest shift in relation to the single nucleon current prediction, but an additional ρ exchange is needed to bring the theory into the data. Also Siegert gives essentially the same quality of agreement. Remarkable are again the strong enhancements at extreme forward and backward angles which unfortunately cannot be checked by available data.

We would like to add the remark that even at $E_d=17.5$ MeV all states for two-nucleon total angular momenta up to at least $j=2$ have to be included. All our calculations are based on up to $j=3$ contributions, which at the higher energies might be not fully converged. In Figs. 33–36 we display the effect of adding the Tuscon-Melbourne 3NF (adjusted to the ^{3}He binding energy). For all observables the effect is negligible if taken together with the Siegert approach. In the case of MEC's, however, the shifts are quite noticeable and move the theory somewhat away from the data in the case of A_{yy} and A_{zz}.

Finally, we demonstrate in Figs. 37–40 that the different *NN* forces taken together with the Siegert approach give essentially the same predictions, which is a feature of robustness of that dynamical picture.

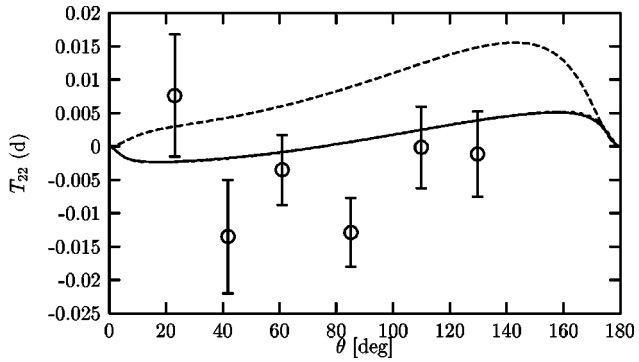

FIG. 25. The same as in Fig. 23 for the tensor analyzing power T_{22}. Data are from [46].

VI. SUMMARY

We have analyzed the angular distributions and some polarization observables in the proton-deuteron radiative cap-

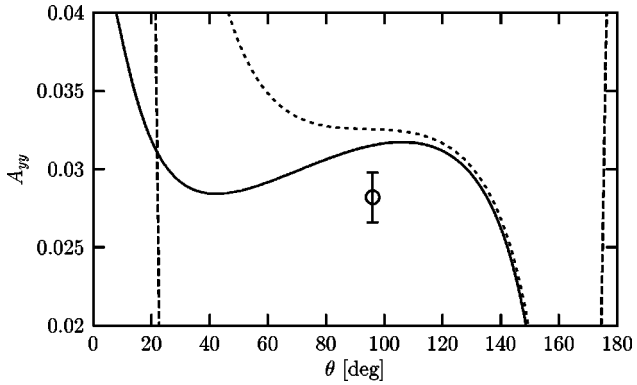

FIG. 27. The tensor analyzing power A_{yy} at $E_d=29.2$ MeV against the c.m. γ-d scattering angle. Curves as in Fig. 7. The data point is from [21].

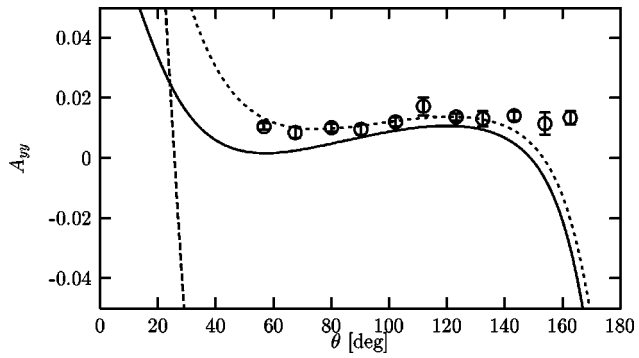

FIG. 28. The tensor analyzing power A_{yy} at $E_d=45$ MeV against the c.m. γ-d scattering angle. Curves as in Fig. 7. Data are from [32].

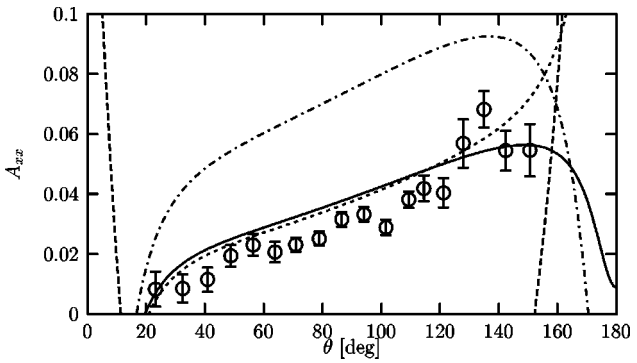

FIG. 30. The tensor analyzing power A_{xx} at $E_d=17.5$ MeV against the c.m. ^{3}He-d scattering angle. Curves as in Fig. 13. Data are from [19].

ture at low and intermediate energies. The corresponding photon lab energy for the inverse photodisintegration process could range from 10 to 140 MeV. We compared the explicit use of MEC's to the use of Siegert's theorem. The MEC's were restricted to π- and ρ-like exchanges as derived from AV18 according to Riska's prescription. The 3N bound and scattering states are rigorous solutions of the adequate Faddeev equations. The calculations are practically converged with respect to angular momentum states except possibly at higher energies. At the lower energies the Siegert and MEC predictions are rather close together. The π-like MEC provides the strongest shift in relation to the single nucleon current towards Siegert's result, but the ρ-like piece is important as another shift. At higher energies the Siegert theorem and MEC's differ in general, which is to be expected since the Siegert approach is mainly active for the lower multipoles.

The agreement with the data is mostly good but there is some room for improvement. Definitely new measurements are needed to improve on certain data sets and to put stronger constraints on the behavior of theoretical predictions at extreme angles. Needless to say, the correct treatment of the initial-state interaction is required in all the cases we studied. PWIA results are very poor (we did not even display them).

The strong and sometimes opposite enhancements of the MEC and Siegert predictions at extreme angles are worthwhile to be mentioned. Precise data would be very useful to rule that out or possibly justify it. In any case if the MEC and the Siegert predictions are opposite, the reason for that should be clarified.

We consider it to be an important result that the different new generation NN force predictions together with the Siegert prediction are very close together, which demonstrates the stability of that dynamical picture. It will be important to investigate in future studies, whether this is also true, when explicit MEC's are used consistently on the NN forces. Here we restricted ourselves to just one case, when working with MEC, the AV18 potential.

Finally, we mention that the inclusion of 3NF's in the form of the Tuscon-Melbourne 2π exchange (adjusted to the ^{3}He binding energy) has only a minor effect in conjunction with the Siegert approach, but a noticeable one (in some cases) if used together with MEC's. Clearly consistency requirements will probably play an essential role and are not the subject of this paper.

ACKNOWLEDGMENTS

This work was supported by the Deutsche Forschungsgemeinschaft (H.K. and J.G.), the Polish Committee for Scientific Research under Grant No. 2P03B03914, and the Science and Technology Cooperation Germany-Poland. W.G. would like to thank the Foundation for Polish Science for financial support during his stay in Cracow. The numerical calcula-

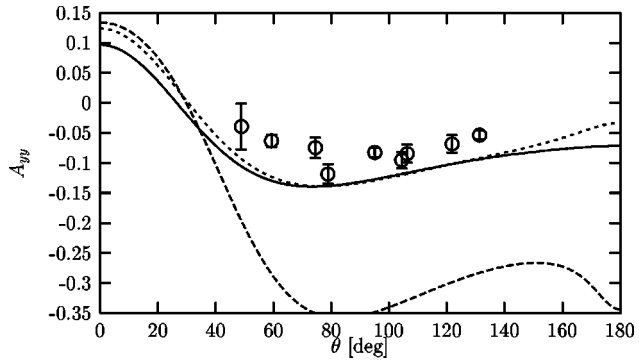

FIG. 29. The same as in Fig. 28 at $E_d=95$ MeV. Data are from [48].

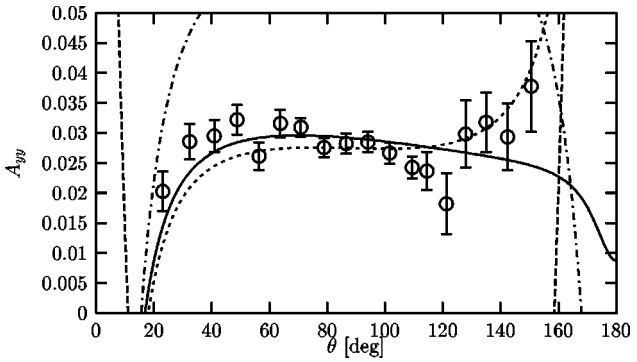

FIG. 31. The same as in Fig. 30 for the tensor analyzing power A_{yy}. Data are from [19].

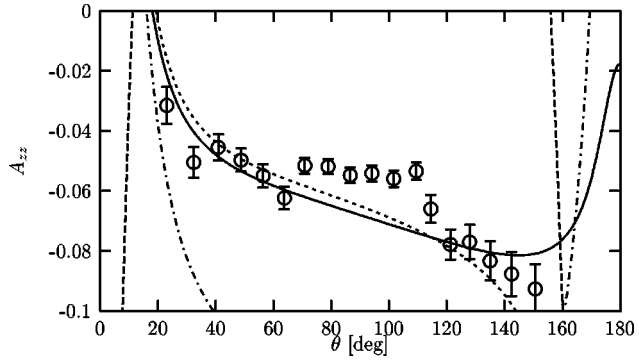

FIG. 32. The same as in Fig. 30 for the tensor analyzing power A_{zz}. Data are from [19].

tions have been performed on the Cray T90 of the NIC in Jülich, Germany.

APPENDIX: AN ALTERNATIVE APPROACH TO THE MULTIPOLE DECOMPOSITION

Here we would like to present an independent derivation of Eq. (8), which differs substantially in technical tools from the one given in Sec. II.

The nuclear matrix elements $\vec{I}(\vec{Q})$ can be expanded in a series of vector spherical harmonics

$$\vec{I}(\vec{Q})=\sum_{lJ\xi} I^{\xi}_{Jl}(Q)\vec{Y}^{*\xi}_{Jl1}(\hat{Q}), \tag{A1}$$

where

$$I^{\xi}_{Jl}(Q)=\int d\hat{Q}'\vec{I}(\vec{Q}')\vec{Y}^{\xi}_{Jl1}(\hat{Q}'). \tag{A2}$$

We denote $Q=|\vec{Q}|=|\vec{Q}'|$. Since l may take the values $l=|J-1|,J,J+1$ in Eq. (A1), we have

$$\vec{I}(\vec{Q})=\sum_{J\xi}\,[I^{\xi}_{JJ-1}(Q)\vec{Y}^{*\xi}_{JJ-11}(\hat{Q})+I^{\xi}_{JJ}(Q)\vec{Y}^{*\xi}_{JJ1}(\hat{Q}) +I^{\xi}_{JJ+1}(Q)\vec{Y}^{*\xi}_{JJ+11}(\hat{Q})]. \tag{A3}$$

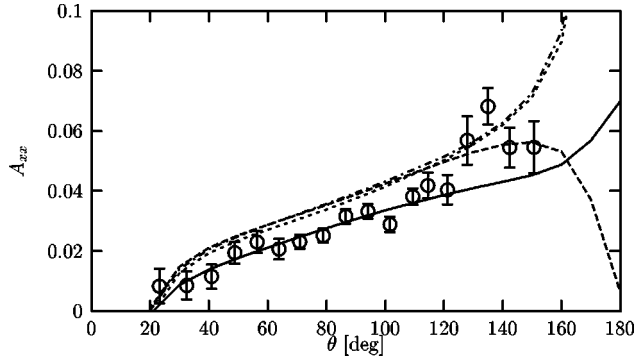

FIG. 33. The tensor analyzing power A_{xx} at $E_d=17.5$ MeV against the c.m. ^{3}He-d scattering angle. Curves as in Fig. 14. Data are from [19].

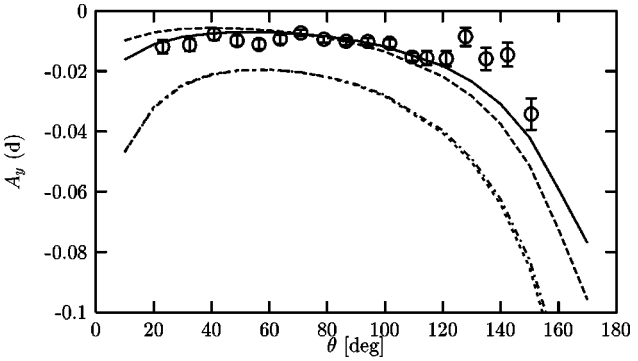

FIG. 34. The same as in Fig. 33 for the deuteron vector analyzing power $A_y(d)$. Data are from [19].

We define

$$\vec{I}^{\,el}_{J\xi}(\vec{Q})=I^{\xi}_{JJ-1}(Q)\vec{Y}^{*\xi}_{JJ-11}(\hat{Q})+I^{\xi}_{JJ+1}(Q)\vec{Y}^{*\xi}_{JJ+11}(\hat{Q}) \tag{A4}$$

and

$$\vec{I}^{\,mag}_{J\xi}(\vec{Q})=I^{\xi}_{JJ}(Q)\vec{Y}^{*\xi}_{JJ1}(\hat{Q}). \tag{A5}$$

In Eqs. (A4) and (A5) we separate terms of electric and magnetic type containing the vector spherical harmonics with parity $(-1)^J$ and $(-1)^{(J+1)}$, respectively,

$$\vec{I}(\vec{Q})=\sum_{J\xi}\,[\vec{I}^{\,el}_{J\xi}(\vec{Q})+\vec{I}^{\,mag}_{J\xi}(\vec{Q})]. \tag{A6}$$

Then we use the following relations [44]:

$$\hat{Q}\times\vec{Y}^{\xi}_{JJ+11}(\hat{Q})=i\sqrt{\frac{J}{2J+1}}\,\vec{Y}^{\xi}_{JJ1}(\hat{Q}), \tag{A7}$$

$$\hat{Q}\times\vec{Y}^{\xi}_{JJ1}(\hat{Q})=i\sqrt{\frac{J+1}{2J+1}}\,\vec{Y}^{\xi}_{JJ-11}(\hat{Q}) +i\sqrt{\frac{J}{2J+1}}\,\vec{Y}^{\xi}_{JJ+11}(\hat{Q}), \tag{A8}$$

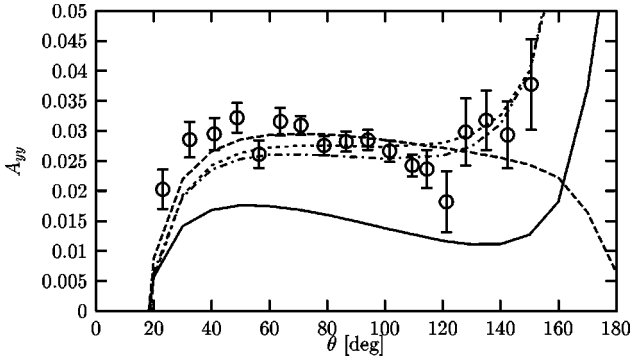

FIG. 35. The same as in Fig. 33 for the tensor analyzing power A_{yy}. Data are from [19].

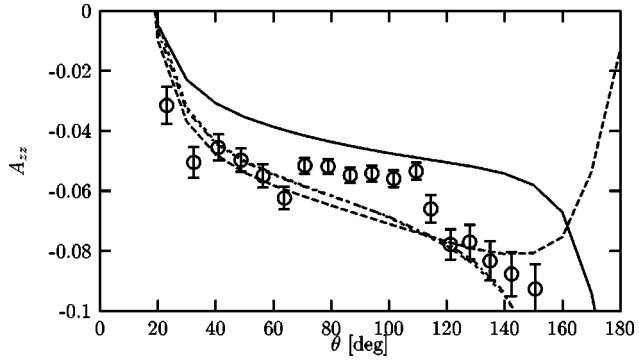

FIG. 36. The same as in Fig. 33 for the tensor analyzing power A_{zz}. Data are from [19].

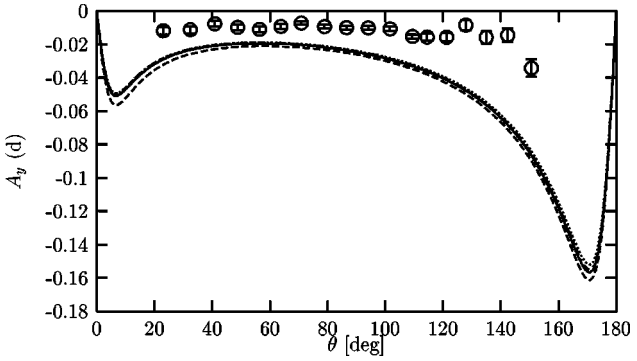

FIG. 38. The same as in Fig. 37 for the deuteron vector analyzing power $A_y(d)$. Data are from [19].

$$\hat{Q}\times\vec{Y}^{\xi}_{JJ-11}(\hat{Q})=i\sqrt{\frac{J+1}{2J+1}}\vec{Y}^{\xi}_{JJ1}(\hat{Q}), \tag{A9}$$

$$\hat{Q}\,Y_{J\xi}(\hat{Q})=\sqrt{\frac{J}{2J+1}}\vec{Y}^{\xi}_{JJ-11}(\hat{Q})-\sqrt{\frac{J+1}{2J+1}}\vec{Y}^{\xi}_{JJ+11}(\hat{Q}), \tag{A10}$$

to derive the following identities:

$$\vec{Y}^{\xi}_{JJ+11}(\hat{Q})=-\sqrt{\frac{J+1}{2J+1}}\hat{Q}\,Y_{J\xi}(\hat{Q})-i\sqrt{\frac{J}{2J+1}}\hat{Q}\times\vec{Y}^{\xi}_{JJ1}(\hat{Q}), \tag{A11}$$

$$\vec{Y}^{\xi}_{JJ-11}(\hat{Q})=\sqrt{\frac{J}{2J+1}}\hat{Q}\,Y_{J\xi}(\hat{Q})-i\sqrt{\frac{J+1}{2J+1}}\hat{Q}\times\vec{Y}^{\xi}_{JJ1}(\hat{Q}). \tag{A12}$$

We use the identities (A11) and (A12) in the angular integrals of Eq. (A2) and get

$$I^{\xi}_{JJ-1}(Q)=\int d\hat{Q}'\vec{I}(\vec{Q}')\vec{Y}^{\xi}_{JJ-11}(\hat{Q}')$$
$$=\int d\hat{Q}'\left[\sqrt{\frac{J}{2J+1}}[\hat{Q}'\cdot\vec{I}(\vec{Q}')]\,Y_{J\xi}(\hat{Q}')+i\sqrt{\frac{J+1}{2J+1}}[\hat{Q}'\times\vec{I}(\vec{Q}')]\cdot\vec{Y}^{\xi}_{JJ1}(\hat{Q}')\right], \tag{A13}$$

$$I^{\xi}_{JJ+1}(Q)=\int d\hat{Q}'\vec{I}(\vec{Q}')\vec{Y}^{\xi}_{JJ+11}(\hat{Q}')$$
$$=\int d\hat{Q}'\left[-\sqrt{\frac{J+1}{2J+1}}[\hat{Q}'\cdot\vec{I}(\vec{Q}')]\,Y_{J\xi}(\hat{Q}')+i\sqrt{\frac{J}{2J+1}}[\hat{Q}'\times\vec{I}(\vec{Q}')]\cdot\vec{Y}^{\xi}_{JJ1}(\hat{Q}')\right]. \tag{A14}$$

Inserting Eqs. (A13) and (A14) into Eq. (A4) and making use of Eqs. (A8) and (A10) leads to

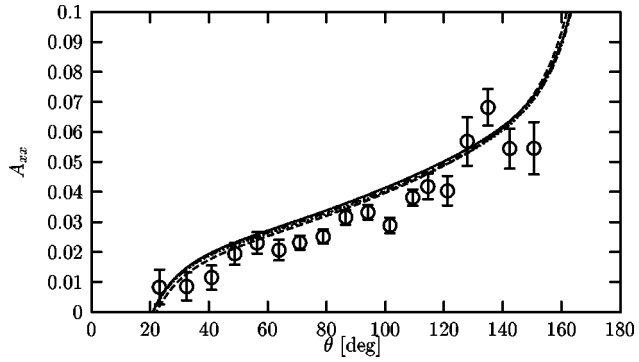

FIG. 37. The tensor analyzing power A_{xx} at $E_d=17.5$ MeV against the c.m. ^{3}He-d scattering angle. Curves as in Fig. 15. Data are from [19].

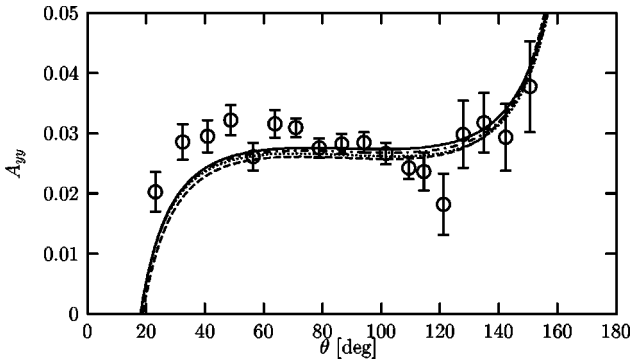

FIG. 39. The same as in Fig. 37 for the tensor analyzing power A_{yy}. Data are from [19].

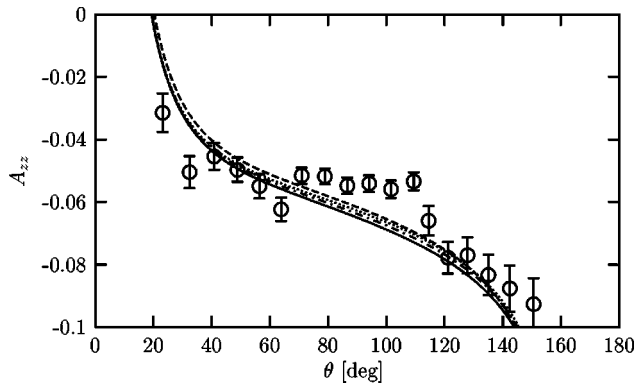

FIG. 40. The same as in Fig. 37 for the tensor analyzing power A_{zz}. Data are from [19].

$$\vec{I}^{el}_{J\xi}(\vec{Q}) = \hat{Q}\, Y^*_{J\xi}(\hat{Q}) \int d\hat{Q}'[\hat{Q}'\cdot\vec{I}(\vec{Q}')]\, Y_{J\xi}(\hat{Q}') - [\vec{Y}^{*\xi}_{JJ1}(\hat{Q})\times\hat{Q}]\int d\hat{Q}'[\hat{Q}'\times\vec{Y}^{\xi}_{JJ1}(\hat{Q}')]\,\vec{I}(\vec{Q}') \equiv \hat{Q}\, Y^*_{J\xi}(\hat{Q})\, 4\pi T^{el}_{J\xi}(Q;long) + i\,[\vec{Y}^{*\xi}_{JJ1}(\hat{Q})\times\hat{Q}] \times 4\pi\, T^{el}_{J\xi}(Q;transv). \quad \text{(A15)}$$

In such a way we introduce the electric transverse

$$T^{el}_{J\xi}(Q;transv) = \frac{i}{4\pi Q}\int d\hat{Q}'[\vec{Q}'\times\vec{Y}^{\xi}_{JJ1}(\hat{Q}')]\cdot\vec{I}(\vec{Q}'), \quad \text{(A16)}$$

and the electric longitudinal multipoles

$$T^{el}_{J\xi}(Q;long) = \frac{1}{4\pi Q}\int d\hat{Q}'(\vec{Q}'\cdot\vec{I}(\vec{Q}'))Y_{J\xi}(\hat{Q}'). \quad \text{(A17)}$$

The magnetic multipoles are defined accordingly

$$T^{mag}_{J\xi}(Q) = \frac{1}{4\pi}\int d\hat{Q}'\,\vec{Y}^{\xi}_{JJ1}(\hat{Q}')\cdot\vec{I}(\vec{Q}'). \quad \text{(A18)}$$

Note that the magnetic multipoles are transverse since $\vec{Q}\cdot\vec{Y}^{\xi}_{JJ1}(\hat{Q}) = 0$. The electric longitudinal multipoles $T^{el}_{J\xi}(Q;long)$ do not appear in our studies of processes with real photons. With the help of the identity

$$\vec{Q}\times\vec{Y}^{\xi}_{JJ1}(\hat{Q}) = i\sqrt{\frac{J+1}{J}}\,\vec{Q}\, Y_{J\xi}(\hat{Q}) + i\sqrt{\frac{2J+1}{J}}\,Q\,\vec{Y}^{\xi}_{J,J+1,1}(\hat{Q}), \quad \text{(A19)}$$

one can introduce a longitudinal term into the expression for the transverse electric multipoles. The aim of this transformation is to get a contribution, which can be associated via the continuity equation

$$\vec{Q}\cdot\vec{I}(\vec{Q}) = \langle\vec{P}'\Psi^{(-)}_f|[H,\hat{\rho}(0)]|\Psi_{^3\mathrm{He}}\vec{P}\rangle = \omega\langle\vec{P}'\Psi^{(-)}_f|\hat{\rho}(0)|\Psi_{^3\mathrm{He}}\vec{P}\rangle = Q\rho(\vec{Q}) \quad \text{(A20)}$$

with the matrix elements of the charge density $\rho(\vec{Q})$. So, the electric multipoles can be cast into the form

$$T^{el}_{J\xi}(Q) = -\frac{1}{4\pi\sqrt{J}}\int d\hat{Q}'[\sqrt{J+1}\,Y_{J\xi}(\hat{Q})\rho(\vec{Q}') + \sqrt{2J+1}\,\vec{Y}^{\xi}_{J,J+1,1}(\hat{Q}')\cdot\vec{I}(\vec{Q}')], \quad \text{(A21)}$$

which is identical to Eq. (8).

Finally, choosing the direction of the z axis along the photon momentum we get for the transverse components of the nuclear matrix element

$$[\vec{I}(Q\vec{e}_z)]_\xi = -\sqrt{2\pi}\sum_{J>1}\sqrt{2J+1}[T^{el}_{J\xi}(Q) + \xi T^{mag}_{J\xi}(Q)], \quad (\xi = \pm 1), \quad \text{(A22)}$$

which coincides with Eq. (2).

[1] V. G. J. Stoks, R. A. M. Klomp, C. P. F. Terheggen, and J. J. de Swart, Phys. Rev. C **49**, 2950 (1994).

[2] R. B. Wiringa, V. G. J. Stoks, and R. Schiavilla, Phys. Rev. C **51**, 38 (1995).

[3] R. Machleidt, F. Sammarruca, and Y. Song, Phys. Rev. C **53**, R1483 (1996).

[4] W. Glöckle, H. Witała, D. Hüber, H. Kamada, and J. Golak, Phys. Rep. **274**, 107 (1996).

[5] H. Witała, W. Glöckle, J. Golak, H. Kamada, and A. Nogga, Proceedings of the XVIth International Conference on Few-Body Problems in Physics, 2000, Taipei, Taiwan, Nucl. Phys. A (to be published).

[6] H. Witała, W. Glöckle, D. Hüber, J. Golak, and H. Kamada, Phys. Rev. Lett. **81**, 1183 (1998).

[7] H. Sakai, K. Sekiguchi, H. Witała, W. Glöckle, M. Hatano, H. Kamada, H. Kato, Y. Maeda, A. Nogga, T. Ohnishi, H. Okamura, N. Sakamoto, S. Sakoda, Y. Satou, K. Suda, A. Tamii, T. Uesaka, T. Wakasa, and K. Yako, Phys. Rev. Lett. **84**, 5288 (2000).

[8] H. Witała, D. Hüber, and W. Glöckle, Phys. Rev. C **49**, R14 (1994).

[9] R. Bieber, W. Glöckle, J. Golak, M. N. Harakeh, D. Hüber, H. Huisman, N. Kalantar-Nayestanaki, H. Kamada, J. G. Messchendorp, A. Nogga, H. Sakai, N. Sakamoto, M. Seip, M.

Volkerts, S. Y. van der Werf, and H. Witała, Phys. Rev. Lett. **84**, 606 (2000).
[10] W. Xu *et al.*, Phys. Rev. Lett. (to be published).
[11] D. Rohe, P. Bartsch, D. Baumann, J. Becker, J. Bermuth, K. Bohinc, R. Böhm, S. Buttazzoni, T. Caprano, N. Clawiter, A. Deninger, S. Derber, M. Ding, M. Distler, A. Ebbes, M. Ebert, I. Ewald, J. Friedrich, J. M. Friedrich, R. Geiges, T. Großmann, M. Hauger, W. Heil, A. Honegger, P. Jennewein, J. Jourdan, M. Kahrau, A. Klein, M. Kohl, K. W. Krygier, G. Kubon, A. Liesenfeld, H. Merkel, K. Merle, P. Merle, M. Mühlbauer, U. Müller, R. Neuhausen, E. W. Otten, Th. Petitjean, Th. Pospischil, M. Potokar, G. Rosner, H. Schmieden, I. Sick, S. Sirca, R. Surkau, A. Wagner, Th. Walcher, G. Warren, M. Weis, H. Wöhrle, and M. Zeier, Phys. Rev. Lett. **83**, 4257 (1999).
[12] W. Glöckle, H. Witała, H. Kamada, J. Golak, A. Nogga, and G. Ziemer, Proceedings of the XVIth International Conference on Few-Body Problems in Physics, [5].
[13] A. Nogga, D. Hüber, H. Kamada, and W. Glöckle, Phys. Lett. B **409**, 19 (1997).
[14] J. Golak, H. Kamada, H. Witała, W. Glöckle, and S. Ishikawa, Phys. Rev. C **51**, 1638 (1995).
[15] V. V. Kotlyar, H. Kamada, J. Golak, and W. Glöckle, Few-Body Syst. **28**, 35 (2000).
[16] A. J. F. Siegert, Phys. Rev. **52**, 787 (1937).
[17] L. L. Foldy, Phys. Rev. **92**, 178 (1953); J. L. Friar and S. Sallieros, Phys. Rev. C **29**, 1645 (1984); J. L. Friar and W. C. Haxton, *ibid.* **31**, 2027 (1985); J. L. Friar and S. Fallieros, *ibid.* **34**, 2029 (1986); **42**, 2246 (1990).
[18] K.-M. Schmitt, P. Wilhelm, H. Arenhövel, A. Cambi, B. Mosconi, and P. Ricci, Phys. Rev. C **41**, 841 (1990); H. Arenhövel, Lect. Notes Phys. **426**, 1 (1994); P. J. Barneo, J. E. Amaro, and A. M. Lallena, Phys. Rev. C **60**, 044615 (1999).
[19] K. Sagara, H. Akiyoshi, S. Ueno, N. Nishimori, A. Motoshima, R. Koyasako, K. Nakashima, T. Fujita, K. Maeda, H. Nakamura, and T. Nakashima, in *Few Body Problems in Physics*, edited by F. Gross, AIP Conf. Proc. No. 334 (AIP, Woodbury, NY, 1995), p. 467; H. Akiyoshi, Ph.D thesis, Kyushu University, 1997.
[20] D. J. Klepacki, Y. E. Kim, and R. A. Brandenburg, Nucl. Phys. **A550**, 53 (1992).
[21] J. Jourdan, M. Baumgartner, S. Burzynski, P. Egelhof, R. Henneck, A. Klein, M. A. Pickar, G. R. Plattner, W. D. Ramsay, H. W. Roser, I. Sick, and J. Torre, Nucl. Phys. **A453**, 220 (1986).
[22] S. Ishikawa and T. Sasakawa, Phys. Rev. C **45**, R1428 (1992).
[23] A. C. Fonseca and D. R. Lehman, Phys. Lett. B **267**, 159 (1991); Few-Body Syst., Suppl. **6**, 279 (1992); Phys. Rev. C **48**, R503 (1993); Few Body Syst. (to be published).
[24] J. L. Friar, B. F. Gibson, and G. L. Payne, Phys. Lett. B **251**, 11 (1990).
[25] A. Kievsky, S. Rosati, and M. Viviani, Nucl. Phys. **A551**, 241 (1993).
[26] J. Carlson and R. Schiavilla, Rev. Mod. Phys. **70**, 743 (1998).
[27] E. A. Wulf, R. S. Canon, S. J. Gaff, J. H. Kelley, R. M. Prior, E. C. Schreiber, M. Spraker, D. R. Tilley, H. R. Weller, M. Viviani, A. Kievsky, S. Rosati, and R. Schiavilla, Phys. Rev. C **61**, 021601(R) (2000).
[28] M. Viviani, R. Schiavilla, and A. Kievsky, Phys. Rev. C **54**, 534 (1996); M. Viviani, A. Kievsky, L. E. Marcucci, S. Rosati, and R. Schiavilla, *ibid.* **61**, 064001 (2000).
[29] D. O. Riska, Phys. Scr. **31**, 107 (1985); **31**, 471 (1985).
[30] T. de Forest, Jr. and J. D. Walecka, Adv. Phys. **15**, 1 (1966); J. D. Walecka, *Theoretical Nuclear and Subnuclear Physics* (Oxford University Press, Oxford, 1995).
[31] J. Golak, H. Witała, H. Kamada, D. Hüber, S. Ishikawa, and W. Glöckle, Phys. Rev. C **52**, 1216 (1995); H. Kamada, W. Glöckle, and J. Golak, Nuovo Cimento A **105**, 1435 (1992).
[32] H. Anklin, L. J. de Bever, S. Buttazzoni, W. Glöckle, J. Golak, A. Honegger, J. Jourdan, H. Kamada, G. Kubon, T. Petitjean, L. M. Qin, I. Sick, Ph. Steiner, H. Witała, M. Zeier, J. Zhao, and B. Zihlmann, Nucl. Phys. **A636**, 189 (1998).
[33] W. Glöckle, J. Golak, H. Witała, and H. Kamada, in *Proceedings of the Elba'98 Workshop on Electron-Nucleus Scattering*, edited by O. Benhar, A. Fabrocini, and R. Schiavilla (Edizioni ETS, Pisa, 1999), pp. 261–274.
[34] W. Glöckle, H. Kamada, J. Golak, H. Witała, S. Ishikawa, and D. Hüber, in *Proceedings of the Second Workshop on Electronuclear Physics with Internal Targets and the BLAST detector*, edited by R. Alarcon and R. Milner (World Scientific, Singapore, 1999), pp. 185–207.
[35] A. R. Edmonds, *Angular Momentum in Quantum Mechanics* (Princeton University Press, Princeton, NJ, 1996).
[36] R. B. Wiringa, R. A. Smith, and T. L. Ainsworth, Phys. Rev. C **29**, 1207 (1994).
[37] D. Hüber, H. Kamada, H. Witała, and W. Glöckle, Acta Phys. Pol. B **28**, 1677 (1997).
[38] S. Galster, H. Klein, J. Moritz, K. H. Schmidt, D. Wegener, and J. Bleckwenn, Nucl. Phys. **B32**, 221 (1971); G. G. Simon, Ch. Schmitt, F. Borkowski, and V. H. Walther, Nucl. Phys. **A333**, 381 (1980).
[39] L. E. Marcucci, D. O. Riska, and R. Schiavilla, Phys. Rev. C **58**, 3069 (1998).
[40] S. A. Coon, M. D. Scadron, P. C. McNamee, B. R. Barrett, D. W. E. Blatt, and B. H. J. McKellar, Nucl. Phys. **A317**, 242 (1979).
[41] W. Sandhas, W. Schadow, G. Ellerkmann, L. L. Howell, and S. A. Sofianos, Nucl. Phys. **A631**, 210c (1998); W. Schadow and W. Sandhas, *ibid.* **A631**, 588c (1998); Phys. Rev. C **59**, 607 (1999).
[42] V. D. Efros, W. Leidemann, G. Orlandini, and E. L. Tomasiuk, Phys. Lett. B **484**, 223 (2000).
[43] R. V. Reid, Ann. Phys. (N.Y.) **50**, 411 (1968).
[44] D. A. Varshalovich, A. N. Moskalev, and V. K. Khersonkii, *Quantum Theory of Angular Momentum* (World Scientific, Singapore, 1988).
[45] A. Amroun, V. Breton, J.-M. Cavedon, B. Frois, D. Goutte, F. P. Juster, Ph. Leconte, J. Martino, Y. Mizuno, X.-H. Phan, S. K. Platchkov, I. Sick, and S. Williamson, Nucl. Phys. **A579**, 596 (1994), and references therein; I. Sick (private communication).
[46] F. Goeckner, W. K. Pitts, and L. D. Knutson, Phys. Rev. C **45**, R2536 (1992).
[47] B. D. Belt, C. R. Bingham, M. L. Halbert, and A. van der Woude, Phys. Rev. Lett. **24**, 1120 (1970).
[48] W. K. Pitts, H. O. Meyer, L. C. Bland, J. D. Brown, R. C. Byrd, M. Hugi, H. J. Karwowski, P. Schwandt, A. Sinha, J.

Sowinski, I. J. van Heerden, A. Arriaga, and F. D. Santos, Phys. Rev. C **37**, 1 (1988).

[49] M. A. Pickar, H. J. Karwowski, J. D. Brown, J. R. Hall, M. Hugi, R. E. Pollock, V. R. Cupps, M. Fatyga, and A. D. Bacher, Phys. Rev. C **35**, 37 (1987).

[50] M. C. Vetterli, J. A. Kuehner, A. J. Trudel, C. L. Woods, R. Dymarz, A. A. Pilt, and H. R. Weller, Phys. Rev. Lett. **54**, 1129 (1985).

[51] G. J. Schmid, R. M. Chastel, H. R. Weller, D. R. Tilley, A. C. Fonseca, and D. R. Lehman, Phys. Rev. C **53**, 35 (1996).